Nano Research
DOI 10.1007/s12274-015-0774-2
Research Article
ISSN 1998-0124
CN 11-5974/O4

Wavelength tunable infrared light emitting diode based on ordered ZnO nanowire/$Si_{1-x}Ge_x$ alloy heterojunction

Taiping Zhang[1,+], Renrong Liang[2,+] (✉), Lin Dong[1], Jing Wang[2] and Jun Xu[2], Caofeng Pan[1] (✉)

Nano Res., **Just Accepted Manuscript** • DOI 10.1007/s12274-015-0774-2
http://www.thenanoresearch.com on March 26, 2015

Just Accepted

TABLE OF CONTENTS (TOC)

Wavelength tunable infrared light emitting diode based on ordered ZnO nanowire/$Si_{1-x}Ge_x$ alloy heterojunction

Taiping Zhang[1,+], Renrong Liang[2,+,*](✉), Lin Dong[1], Jing Wang[2,] and Jun Xu[2,], Caofeng Pan[1,*] (✉)

1. Beijing Institute of Nanoenergy and Nanosystems, Chinese Academy of Sciences, Beijing, China, 100083

2. Institute of Microelectronics, Tsinghua University, Beijing, China, 100084.

+ Authors contributed equally to this work.

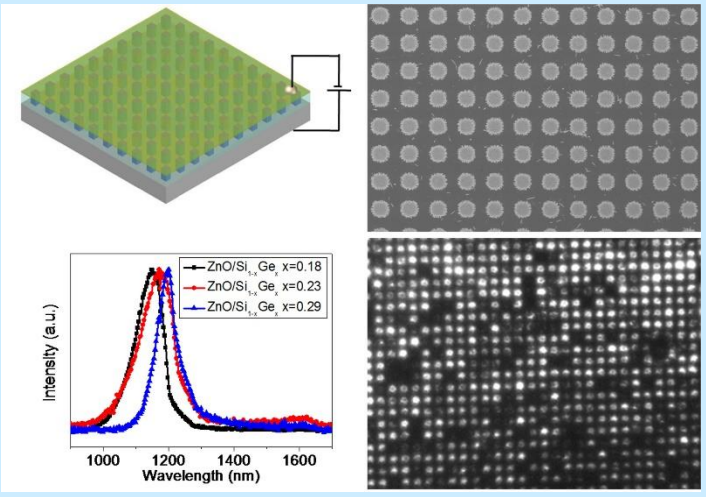

This work provides a novel wavelength tunable infrared light emitting diode based on ZnO nanowire/SiGe alloy heterojunctions. The electroluminescence wavelength of the LED is tuned by the Si and Ge compositions of the SiGe alloy.

Caofeng Pan, cfpan@binn.cas.cn http://piezotronics.binncas.cn/

Renrong Liang, liangrr@mail.tsinghua.edu.cn

Nano Res.

DOI (automatically inserted by the publisher)
Research Article

Wavelength tunable infrared light emitting diode based on ordered ZnO nanowire/$Si_{1-x}Ge_x$ alloy heterojunction

Taiping Zhang[1,+], Renrong Liang[2,+,*] (✉), Lin Dong[1], Jing Wang[2,] and Jun Xu[2,], Caofeng Pan[1,*] (✉)

1. Beijing Institute of Nanoenergy and Nanosystems, Chinese Academy of Sciences, Beijing, China, 100083
2. Institute of Microelectronics, Tsinghua University, Beijing, China, 100084.
Address correspondence to: cfpan@binn.cas.cn, liangrr@tsinghua.edu.cn
+ Authors contributed equally to this work.

ABSTRACT

We proposed and developed a novel infrared light emitting diode (LED) based on ordered p-n heterojunction built of p-$Si_{1-x}Ge_x$ alloy and n-ZnO nanowires. The Electroluminescence (EL) emission of this LED is in the infrared range, which is dominated by the band gap of $Si_{1-x}Ge_x$ alloy. The EL wavelength variation of the LED shows a red shift depends on the increasing of Ge content. With the Ge compositions of 0.18, 0.23 and 0.29, the average EL wavelengths are around 1144 nm, 1162 nm and 1185 nm, respectively. The amplitude of red shift matched with the theoretical calculation. Therefore, by modulating the Ge composition of the $Si_{1-x}Ge_x$ alloy, we can adjust the band gap of the SiGe film and tune the emission wavelength of the fabricated LED. Such IR LED device may have great potential applications in optical communication, environmental monitoring and biological and medical analyses.

KEYWORDS

ZnO nanowire, SiGe alloy, infrared light emitting diode, wavelength tunable

1 Introduction

Semiconductor nanowires have attracted more and more interests for their promising applications in optoelectronics. A branch of these applications is light emitting diode (LED) device. Compared with the devices based on thin films[1-3], nanowire-based LED could not only avoid the total internal reflection between the films but also have higher extraction efficiency by means of the nanowire's waveguiding property[4-6]. ZnO nanowire is regarded as one of the most promising materials for next generation optoelectronics due to its large exciton binding energy and wide direct bandgap energy at room temperature[7]. Since the fabrication of high quality p-ZnO is still confronting great challenges to form p-n homojuncion[8, 9], ZnO LED based on heterojunction including p-GaN/n-ZnO, p-polymer/n-ZnO and p-Si/n-ZnO were investigated as alternative structures[10-16].

Si is a traditional semiconductor material in the integrated circuit industry. The ZnO/Si LED nanodevices have been studied widely, from single wire LED to nanowires or nanorods array LED[17-25]. However, most studies focused on the electroluminescence (EL) emitting of these devices in visible range. Research on EL emitting in infrared (IR) range had been neglected until Chen's group reported an IR EL emitting from ZnO/Si-nanotip LED in 2009[26]. The IR wavelength corresponds to Si band gap energy. Their work opens a door that induces researchers move attention to the IR emitting of ZnO/Si heterojunction. In C, Si, and Ge element family, SiGe alloy takes a unique place because its band gap can vary smoothly from Si (about 1.155 eV) to Ge band gap (about 0.740 eV), which depends on the Si and Ge atomic percentages[27-30]. Therefore, a marriage between ZnO and SiGe alloy could realize a new wavelength tunable IR LED device, which has attracted more and more attentions in recent years[31-34]. Same as other IR LED nanodevice, this novel device may have great potential applications in optical communication, environmental monitoring and biological and medical analyses[35, 36]. In addition, ordered nanowires LED has a better prospect than random distributed nanowires LED [10].

In this work, we demonstrate the first exploration of design, fabrication and characterization of ordered LED devices, which are formed by p-type $Si_{1-x}Ge_x$ alloy (x = 0.18, 0.23 and 0.29) and n-type ZnO nanowires ordered array heterojunction. Each LED consists of multi n-ZnO nanowires/p-SiGe LED diodes with 15 μm pitch, corresponding to a pixel density of 3175 dpi. The EL spectrum reveals that the LEDs generate an IR emission, which corresponds to the corresponding SiGe band gap. The emission wavelength has an obvious red shift as the Ge content increases. Corresponding to the Ge composites of 0.18, 0.23 and 0.29, the EL peak arises from 1144 nm, 1162 nm, to 1185 nm, and such red shift matches well with the theoretical

calculation. The developed techniques could pave the way for exploring new functions of SiGe based optoelectronic nanodevices.

2 Experimental Sections

The proposed LED device based on ordered ZnO nanowire/$Si_{1-x}Ge_x$ alloy heterojunction contains a heavily doped p-type $Si_{1-x}Ge_x$ layer (carrier density of 1019 cm^{-3}) and an ordered n-type ZnO nanowire pixels array. A schematic of the fabrication process is presented in figure 1a. Frist, strained $Si_{1-x}Ge_x$ (x = 0.18, 0.23 and 0.29) layer was grown on p-type lightly doped 8 inch (001) Si wafers (resistivity of 1-20 Ω·cm) using an Applied Material Epi Centura 200 RPCVD system (figure 1ai). Second, a UV-lithography was employed to generate a patterned template of a negative photoresist over the $Si_{1-x}Ge_x$ layer, which was consisted of squares with 5 μm side and 15 μm pitch of each square. Third, a thin film of polycrystalline ZnO seed was deposited by magnetron sputtering on the $Si_{1-x}Ge_x$ layer and photoresist template. After the lift-off process, the ZnO seed squares array only leave on the $Si_{1-x}Ge_x$ layer of the photoresist holes (figure 1aii). Then, a hydrothermal growth method was used to synthesize the ZnO nanowire pixels (figure 1aiii). Next, a layer of SU8 photoresist was spun coated to wrap around the ZnO nanowire pixels. The top part of the photoresist was etched by oxygen plasma to expose the tips of the nanowires (figure 1aiv). Finally, a layer of indium tin oxide (ITO) was sputtered on the top of the device to work as top electrode (figure 1av).

3 Results and discussion

Figures 1b to 1e show the typical SEM images of the ZnO nanowire arrays grown on the SiGe layer after hydrothermal growth process, the LEDs with ITO electrode and the cross-section of the ZnO/SiGe heterojunction, respectively. Here we present the results of ZnO/ $Si_{0.71}Ge_{0.29}$ heterojunction structure for a typical example. As shown in the insert image in figure 1b, because the surrounding nanowires provide certain spatial confinement, the nanowires in the middle of the pixels have good alignment and are perpendicular to the SiGe plane. From the insert image that zooms on the top of a pixel, we can observe the hexagonal tops of the ZnO nanowires. The SEM image (presented in figure 1c) of the LED device shows that all the nanowire pixels are wrapped by the SU8 photoresist, and that the heads of the nanowires are exposed after the oxygen plasma etching. Each pixel is a single LED that works as a pixel of the device. Through the cross-sectional SEM image of the nanowire pixels and SiGe layer, we can observe that the ZnO nanowires are around 2 μm high, as shown in figure 1d. Figure 1e presents the enlarged SEM image of the interface between a single ZnO nanowire pixel and the Si substrate, the SiGe layer can be clearly seen and its thickness is about 40 nm.

To reveal the construction of the p-n heterojunction, we carried out a series of characterization

measurement on the ordered ZnO nanowire/$Si_{1-x}Ge_x$ alloy nano-system. Figure 2a shows the X-ray diffraction (XRD) spectra of ZnO nanowires on the SiGe layers with three different Ge compositions. The ZnO (100), ZnO (002), ZnO (101), ZnO (101), ZnO (102), ZnO (110) ZnO (103) and ZnO (004) peaks are observed at 31.7°, 34.4°, 36.2°, 47.5°, 56.6°, 62.8° and 72.5°, confirming a wurtzite-type ZnO crystal [23, 37, 38]. The strongest peak located at 34.4° that indexed as (002) indicates the ZnO nanowires are preferentially oriented in the c-axis direction and most of the nanowires are perpendicular to the SiGe layer [12, 17, 24, 38]. These results are consistent with the SEM measurement described above. We also find Si (004) at 69.13° and SiGe (004) peaks close to it on low degree side. As shown in figure 2b, the SiGe (004) peak position moves toward lower degree angle along with the increasing of Ge composition ($Si_{0.82}Ge_{0.18}$ at 68.0°, $Si_{0.77}Ge_{0.23}$ at 67.8° and $Si_{0.71}Ge_{0.29}$ at 67.6°). The thicknesses of the strained SiGe layer can be calculated from the interference fringes, which are approximately 24 nm, 28 nm and 40 nm for $Si_{0.82}Ge_{0.18}$, $Si_{0.77}Ge_{0.23}$ and $Si_{0.71}Ge_{0.29}$ layers, respectively. The growth of high quality SiGe alloys using RPCVD system is a mature manufacturing technique in semiconductor technology, including the precise control of Ge composition, strain state, film and surface morphology of the SiGe layers[39, 40].

Figure 2c shows the Raman spectra of the three ZnO nanowire/SiGe heterostructure. The Raman spectra were collected with a micro-Raman spectrometer (HR Evolution, Jobin Yvon) excited by a 532 nm laser at 50 mW. The scatterings of the SiGe alloy and the ZnO nanowires are clearly observed. The scattering peak at 520 cm^{-1} is attributed to the first-order optical phonons of Si-Si bond [41], while that at 414 cm^{-1} is assigned to optic phonons involving Si-Ge stretching motions [42-44]. The two sharp peaks at 99 and 438 cm^{-1} correspond to the low–frequency and high-frequency E_2 modes of ZnO, respectively[45, 46]. The Raman peak at about 300 cm^{-1} consists of two vibration modes: Ge-Ge stretching motions centered at 290 cm^{-1} and Si-Si 2TA mode at 302 cm^{-1} [41-44]. The intensity of Raman peak at about 290 cm^{-1}, which corresponds to the Ge-Ge mode, rises along with the Ge content increase, whereas the relative intensity of Si-Si 2TA mode at 302 cm^{-1} keeps unchanged. For the SiGe alloys with different Ge contents, the positions of the ZnO E_2(high) modes are same as the bulk ZnO, indicating the ZnO nanowires are free of stress [46]. Meanwhile, there are three weak Raman peaks at 333, 378 and 572 cm^{-1}, which are assigned to the second order scattering (E_2(high)-E_2(low) mode), A_1(TO) mode , and A_1(LO) mode of ZnO, respectively [45, 46].

The photoluminescence (PL) spectra of the ZnO nanowire/SiGe alloys were obtained. The PL spectra were performed by excitation from a 500 W Xe lamp and the exciting wavelength was set to be 325 nm (FLS980, Edinburgh Instruments). The PL emission was collected by a photomultiplier tube in

UV-visible range. From the PL spectra shown in figure 2d, we can see that all the ZnO nanowires of the three structures have a narrow peak at around 380 nm in U-V range and a wide peak at about 620 nm in visible range. The U-V peak corresponds to the near-band-edge emission, while the visible peak is usually attributed to defects such as oxygen vacancies and zinc interstitials [17-19, 22, 24, 26]. The PL spectra indicate that the ZnO nanowires grown on different $Si_{1-x}Ge_x$ alloy layers have similar PL emission mechanisms.

The current-voltage (I-V) characteristics of the three types of LED devices with the same sizes (5 mm × 5 mm) are plotted in figure 3a. All of the devices exhibit obvious rectification behavior with threshold voltages of the devices around 6.5V, indicating high-quality p-n heterojunctions formed between the ZnO nanowires and the SiGe alloy layer. The increase of Ge composition does not strongly influence the rectification property of the devices. Figure 3b shows an typical optical image of a lighted-up ZnO nanowire/$Si_{0.71}Ge_{0.29}$ alloy LED device, the applied current is set to be 0.3 A, corresponding to an current density of 0.12 mA/cm^2. The image was picked by an objective equipped on a commercial microscope (Axio Observer. Z1, Zeiss). The ordered array can be clearly seen with the designed pixel density of 3175 dpi (15 μm pitches). The light intensity profile of five adjacent representative LEDs that are marked by a white rectangle is show in figure 3c, together with the corresponding LED devices. The profile does not show crosstalk between the adjacent LEDs.

The most important characterization of the LEDs is the electroluminescence (EL) spectra, which were measured at room temperature (NIR1700 spectrometer, Ideaoptics). Infrared EL (IR EL) spectra for the three types of LED devices are plotted as a function of the applied current, as shown in figure 4b, 4d and 4f. All the three devices display a strong and narrow peak in range of 1140 nm to 1200 nm, which corresponds to the energy band of the SiGe alloy. For each device, the EL intensity increases with the increase of the applied current. And the peak position has slightly red shift corresponds to the increasing of current. The bathochromic shift of electroluminescence may be caused by the joule heat affect, as reported by Chen et.al. [26]. In addition, a very weak visible EL peak are observed from the developed devices with high applied current intensity, which are located at the shoulder of the IR EL peak, as shown in figure 4a, 4c, and 4e (QE65 Pro spectrometer, Ocean Optics). The EL curves of all devices have the same general features, extending from 450 nm to beyond 900 nm and being centered at about 700 nm. This visible EL phenomenon is believed to be due to the defects and surface states of ZnO, in accordance with visible PL emission[18, 19, 22, 24].

As discussed above, the IR EL emitting of the fabricated LED devices is attributed to the band edge emitting of the binary SiGe alloy. To understand the relationship between the Ge

composition and the EL emitting wavelength, we compare the EL spectra of devices with different Ge contents. A three dimensional (3D) graph of the wavelength shift along the Ge composition and applied current is plotted in figure 5a. An overall trend of how wavelength move with the change of the two factors can be simultaneously derived from this 3D graph. Figure 5b shows the wavelength variations of three devices with the Ge composition of 18%, 23% and 29%. We can see a clearly red shift corresponds to the increasing of Ge content. As described in Ref. 27, the energy band gap of $Si_{1-x}Ge_x$ alloy varies smoothly from the Si energy band gap at 1.155 eV to the band gap in Ge at 0.740 eV depends on the factor x, an alternation from the Si-like X-conduction-band minimum to the Ge-like L-conduction-band minimum occurs at until x = 0.85. Theoretically, by using the tight-binding method within the virtual crystal approximation, the energy band between the top at Γ of the valence band and the X, L or Γ point in the conduction band of a $Si_{1-x}Ge_x$ alloy can be deduced by equation 1 by:

$$E_g^{SiGe} = (1-x)E_g^{Si} + xE_g^{Ge} + b_{SiGe}x(1-x) \quad (1)$$ [30].

However, the bowing parameter *bSiGe* is difficult to determine here. Therefore, we employ the fitting calculation from Ref. 27. Since the SiGe alloy layers are grown on the Si substrate, they should have a "Si-like" band structure [29]. Hence we use the calculation for the Si-like X band:

$$E_g^{SiGe}(x) = 1.155 - 0.43x + 0.206x^2 \quad \text{eV} \quad (2)$$ [27].

The energy band gap of the three compositions SiGe alloy layers are 1.084 eV for factor x 0.18, 1.067 eV for 0.23 and 1.048 eV for 0.29, corresponding to the emitting wavelength at 1144 nm, 1162 nm and 1184 nm, respectively. Figure 5c shows the emitting peaks variations of the three devices as a function of the applied currents. The average emitting wavelength is around 1144 nm, and 1162 nm and 1185 nm for the fabricated LED devices with $Si_{0.82}Ge_{0.18}$, $Si_{0.77}Ge_{0.23}$ and $Si_{0.71}Ge_{0.29}$ alloy, respectively. The measurement results match well with the theoretical calculation. These results strongly indicate that the SiGe alloy band edge emitting dominates the IR EL emitting of the developed LED devices. By adjusting the relative composition of Si and Ge elements, we can manipulate the energy band gap of SiGe alloy and then tune the emitting wavelength of the ZnO/SiGe heterojunction LED. Hence the proposed idea that a marriage between ZnO and SiGe alloy could realize a new wavelength tunable IR LED device is confirmed. Figure 5c shows the wavelength variations of the three devices under different applied currents. For all devices, the wavelength of the EL peak exhibits obvious batho-shift when the applied current exceeds 0.10 A, which is attributed to the joule heat effect. When the applied currents are lower than 0.10 A, the heat dissipation via conduction and radiation may counteract the accumulation of the joule heat by the device. Further increase in the applied current from 0.10 A to 0.25 A will cause obvious rising in the device

temperature, hence resulting in the red shift of wavelength.

4 Conclusions

In conclusion, we have demonstrated a novel NW LEDs array based on ordered ZnO nanowire/SiGe alloy heterojunction arrays. It is shown that the LED device has IR emitting, which is dominated by SiGe band edge emitting. Through adjusting the Ge composition of the SiGe alloy, we can modulate the energy bandgap of the SiGe alloy and further tune the emitting wavelength of the LED device. The developed LED device is compactable with conventional Si based integrated circuit technology and may open an avenue for design, fabrication and application of a new generation of micro/nano wavelength tunable IR light sources or display device. The developed techniques may have wide potential of applications in integration optoelectronics, telecommunication, optical interconnect systems and IR sensor areas.

Acknowledgements

The authors are grateful for the support from the "Thousands Talents" program for pioneer researcher and his innovation team, China; President Funding of the Chinese Academy of Sciences, National Natural Science Foundation of China (No.51272238, 21321062, 51432005 and 61405040), the Innovation Talent Project of Henan Province (No. 13HASTIT020), Talent Project of Zhengzhou Univ (ZDGD13001) and Surface Engineering Key Lab of LIPCAST; Tsinghua University Initiative Scientific Research Program, National Natural Science Foundation of China (No.61306105).

References

[1] Vispute, R. D.; Talyansky, V.; Choopun, S.; Sharma, R. P.; Venkatesan, T.; He, M.; Tang, X.; Halpern, J. B.; Spencer, M. G.; Li, Y. X. et al. Heteroepitaxy of ZnO on GaN and its implications for fabrication of hybrid optoelectronic devices. Appl. Phys. Lett. 1998, 73, 348-350.

[2] Alivov, Ya. I.; Van Nostrand, J. E.; Look, D. C.; Chukichev, M. V.; Ataev, B. M. Observation of 430 nm electroluminescence from ZnO/GaN heterojunction light-emitting diodes. Appl. Phys. Lett. 2003, 83, 2943-2945.

[3] Asıl, H.; Gür, E.; Çınar, K.; Coşkun, C. Electrochemical growth of n-ZnO onto the p-type GaN substrate: p-n heterojunction characteristics. Appl. Phys. Lett. 2009, 94, 253501.

[4] Zhong, J.; Chen, H.; Saraf, G.; Lu, Y; Choi, C. K.; Song J. J.; Mackie, D. M.; Shen, H. Integrated ZnO nanotips on GaN light emitting diodes for enhanced emission efficiency. Appl. Phys. Lett. 2007, 90, 203515.

[5] An, S. J.; Chae, J. H.; Yi, G-C.; Park, G. H. Enhanced light output of GaN-based light-emitting diodes with ZnO nanorod arrays. Appl. Phys. Lett. 2008, 92, 121108.

[6] Kim, K. S.; Kim, S-M.; Jeong, H.; Jeong, M. S.; Jung, G. Y. Enhancement of light extraction through the wave-guiding effect of ZnO sub-microrods in InGaN

blue light-emitting diodes. Adv. Funct. Mater. 2010, 20, 1076-1082.

[7] Alivov, Ya. I.; Kalinina E. V.; Cherenkov, A. E.; Look, D. C.; Ataev, B. M.; Omaev A. K.; Chukichev, M. V.; Bagnall, D. M. Fabrication and characterization of n-ZnO/p-AlGaN heterojunction light-emitting diodes on 6H-SiC substrates. Appl. Phys. Lett. 2003, 83, 4719-24721.

[8] Look, D. C.; Claflin, B.; Alivov, Ya. I.; Park, S. J. The future of ZnO light emitters. Phys. Stat. Sol. (a) 2004, 201, 2203-2212.

[9] Xiang, B.; Wang, P.; Zhang, X.; Dayeh, S. A.; Aplin, D. P. R.; Soci, C.; Yu, D.; Wang, D. Rational synthesis of p-type zinc oxide nanowire arrays using simple chemical vapor deposition. Nano Lett. 2007, 7, 323-328.

[10] Xu, S.; Xu, C.; Liu, Y.; Hu, Y.; Yang, R.; Yang, Q.; Ryou, J-H.; Kim, H. J.; Lochner, Z.; Choi, S. et al. Ordered nanowire array blue/near-UV light emitting diodes. Adv. Mater. 2010, 22, 4749-4753.

[11] Jha, S.; Qian, J-C.; Kutsay, O.; Jr, J. K.; Luan, C-Y.; Zapien, J. A.; Zhang, W.; Lee, S-T.; Bello, I. Violet-blue LEDs based on p-GaN/n-ZnO nanorods and their stability. Nanotechnology 2011, 22, 245202.

[12] Zhang, S. G.; Zhang, X. W.; Si, F. T.; Dong, J. J.; Wang, J. X.; Liu, X.; Yin, Z. G.; Gao, H. L. Ordered ZnO nanorods-based heterojunction light-emitting diodes with grapheme current spreading layer. Appl. Phys. Lett. 2012, 101, 121104.

[13] Pan, C.; Dong, L.; Zhu, G.; Niu, S.; Yu, R.; Yang, Q.; Liu, Y.; Wang, Z. L. High-resolution electroluminescent imaging of pressure distribution using a piezoelectric nanowire LED array. Nat. Photon. 2013, 7, 752-758.

[14] Yang,Q.; Wang, W.; Xu, S.; Niu, S.; Wang, Z. L. Enhancing light emission of ZnO microwire-based diodes by piezo-phototronic effect. Nano Lett. 2011, 11, 4012-4017.

[15] Yang, Q.; Liu, Y.; Pang, C.; Chen, J.; Wen, X.; Wang, Z. L. Largely enhanced efficiency in ZnO nanowire/p-polymer hybridized inorganic/organic ultraviolet light-emitting diode by piezo-phototronic effect. Nano Lett. 2013, 13, 607-613.

[16] Wang, C.; Bao, R.; Zhao, K.; Zhang, T.; Dong, L.; Pan, C. Enhanced emission intensity of vertical aligned flexible ZnO nanowire/p-polymer hybridized LED array by piezo-phototronic effect. Nano Energy. Doi: 10.1016/j.nanoen.2014.11.033.

[17] Sun, H.; Zhang, Q-F.; Wu, J-L. Electroluminescence from ZnO nanorods with an n-ZnO/p-Si heterojunction structure. Nanotechnology 2006, 17, 2271-2274.

[18] Bao, J.; Zimmler, M. A.; Capasso, F. Broadband ZnO single-nanowire light-emitting diode. Nano Lett. 2006, 6, 1719-1722.

[19] Chen, P.; Ma, X.; Yang, D. Ultraviolet electroluminescence from ZnO/p-Si heterojunctions. J. Appl. Phys. 2007, 101, 053103.

[20] Zimmler, M. A.; Voss, T.; Ronning, C.; Capasso, F. Exciton-related electroluminescence from ZnO nanowire light-emitting diodes. Appl. Phys. Lett. 2009, 94, 241120.

[21] Lee, S. W.; Cho, H. D.; Panin, G.; Kang, T. W. Vertical ZnO nanorod/Si contact light-emitting diode. Appl. Phys. Lett. 2011, 98, 093110.

[22] Jung, B. O.; Lee, J. H.; Lee, J. Y.; Kim, J. H.; Cho, H. K. High-purity ultraviolet electroluminescence from n-ZnO nanowires/p+-Si heterostructure LEDs with i-MgO film as carrier control layer. J. Electrochem. Soc. 2012, 159, H102-H106.

[23] Chan, Y. F.; Su, W.; Zhang, C. X.; Wu, Z. L.; Tang, Y.; Sun, X. Q.; Xu, H. J. Electroluminescence from ZnO-nanofilm/Si-micropillar heterostructure arrays. Opt. Express 2012, 20, 24280-24287.

[24] Tsai, J. K.; Shih, J. H.; Wu, T. C.; Meen, T. H. n-ZnO nanorods/p+-Si (111) heterojunction light emitting diodes. Nanoscale Res. Lett. 2012, 7, 664.

[25] Xian, F.; Wang, X.; Xu, L.; Li, X.; Bai, W. Color tunable electroluminescence from Co-doped ZnO nanorods/p-Si heterojunction. J. Lumin. 2013, 144, 154-157.

[26] Hsieh, Y-P.; Chen, H-Y.; Lin, M-Z.; Shiu, S-C.; Hofmann, M.; Chern, M-Y.; Jia, X.; Yang, Y-J.; Chang, H-J.; Huang, H-M. et al. Electroluminescence from

ZnO/Si-nanotips light-emitting diodes. Nano Lett. 2009, 9, 1839-1843.

[27] Weber, J.; Alonso, M. I. Near-band-gap photoluminescence of Si-Ge alloys. Phys. Rev. B 1989, 40, 5683-5693.

[28] Rieger, M. M.; Vogl, P. Electronic-band parameters in strained $Si_{1-x}Ge_x$ alloys on $Si_{1-y}Ge_y$ substrates. Phys. Rev. B 1993, 48, 14276-14287.

[29] Fischetti, M. V.; Laux, S.E. Band structure, deformation potentials, and carrier mobility in strained Si, Ge, and SiGe alloys. J. Appl. Phys. 1996, 80, 2234-2252.

[30] Moontragoon, P.; Ikonić, Z.; Harrison, P. Band structure calculations of Si-Ge-Sn alloys: achieving direct band gap materials. Semicond. Sci. Technol. 2007, 22, 742-748.

[31] Li, J.; Meng, C.; Liu, Y.; Wu, X.; Lu, Y.;Ye, Y.; Dai, L.; Tong, L.; Liu, X.; Yang, Q. Wavelength tunable CdSe nanowire laser based on the absorption-emission-absorption process. Adv. Mater. 2013, 25, 833-837.

[32] Yang, Z.; Wang, D.; Meng, C.; Wu, Z.; Wang, Y.; Ma, Y.; Dai, L.; Liu, X.; Hasan, T.; Liu, X. et al. Broudly defining lasing wavelengths in single bandgap-graded semiconductor nanowire. Nano. Lett. 2014, 14, 3153-3159.

[33] Tsang, M-K.; Bai, G.; Hao, J. Stimuli responsive upconversion luminescence nanomaterials and films for various applications. Chem. Soc. Rev. 2015, 44, 1585-1607.

[34] Bai, G.; Tsang, M-K.; Hao, J. Tuning the luminescence of phosphors: beyond conventional chemical method. Adv. Optical Mater. Doi: 10.1002/adom.201400375.

[35] Han, C. B.; He, C.; Li, X. J. Near-infrared light emission from a GaN/Si nanoheterostructure array. Adv. Mater. 2011, 23, 4811-4814.

[36] Han, C. B.; He, C.; Meng, X. B.; Wan, Y. R.; Tian, Y. T.; Zhang, Y. J.; Li, X. J. Effect of annealing treatment on electroluminescence from GaN/Si nanoheterostructure array. Opt. Express 2012, 20, 5636-5643.

[37] Li, Y.; Meng, G. W.; Zhang, L. D.; Phillipp, F. Ordered semiconductor ZnO nanowire arrays and their photoluminescence properties. Appl. Phys. Lett. 2000, 76, 2011-2013.

[38] Zhang, R.; Yin, P-G.; Wang, N.; Guo, L. Photoluminnescence and raman scattering of ZnO nanorods. Solid state Sci. 2009, 11, 865-869.

[39] Hartmann, J. M.; Bogumilowicz, Y.; Holliger, P.; Laugier, F.; Truche, R.; Rolland, G.; Séméria, M. N.; Renard, V.; Olshanetsky, E. B.; Estibals, O. et al. Reduced pressure chemical vapour deposition of SiGe virtual substrates for high mobility devices. Semicond. Sci. Technol. 2004, 19, 311-318.

[40] Liang, R.; Zhang, K.; Yang, Z.; Xu, Y.; Wang, J.; Xu, J. Fabrication and characterization of strained Si material using SiGe virtual substrate for high mobility devices. J. Semicond. 2007, 28, 1518-1522.

[41] Li, B.; Yu, D.; Zhang, S-L. Raman spectral study of silicon nanowires. Phys. Rev. B 1999, 59, 1645-1648.

[42] Winer, K.; Alonso, M. I. Raman spectra of c-$Si_{1-x}Ge_x$ alloys. Phys. Rev. B 1989, 39, 10056-10062.

[43] Torres, V. J. B.; Coutinho, J.; Briddon, P. R.; Barroso, M. Ab-initio vibrational properties of SiGe alloys. Thin Solid films 2008, 517, 395-397.

[44] Pagès, O.; Souhabi, J.; Torres V. J. B.; Postnikov, A. V.; Rustagi, K. C. Re-examination of the SiGe raman spectra: percolation/one-dimensional-pixel scheme and ab initio calculations. Phys. Rev. B 2012, 86, 045201.

[45] Cuscó, R.; Alarcón-Lladó, E.; Ibáñez, J.; Artús, L.; Jiménez, J.; Wang, B.; Callahan, M. J. Temperature dependence of raman scattering in ZnO. Phys. Rev. B 2007, 75, 165202.

[46] Huang, Y.; Liu, M.; Li, Z.; Zeng, Y.; Liu, S. Raman spectroscopy study of ZnO-based ceramic films fabricated by novel sol-gel process. Mat. Sci. Eng. B 2003, 97, 111-116.

Figures and figure captions

Figure 1

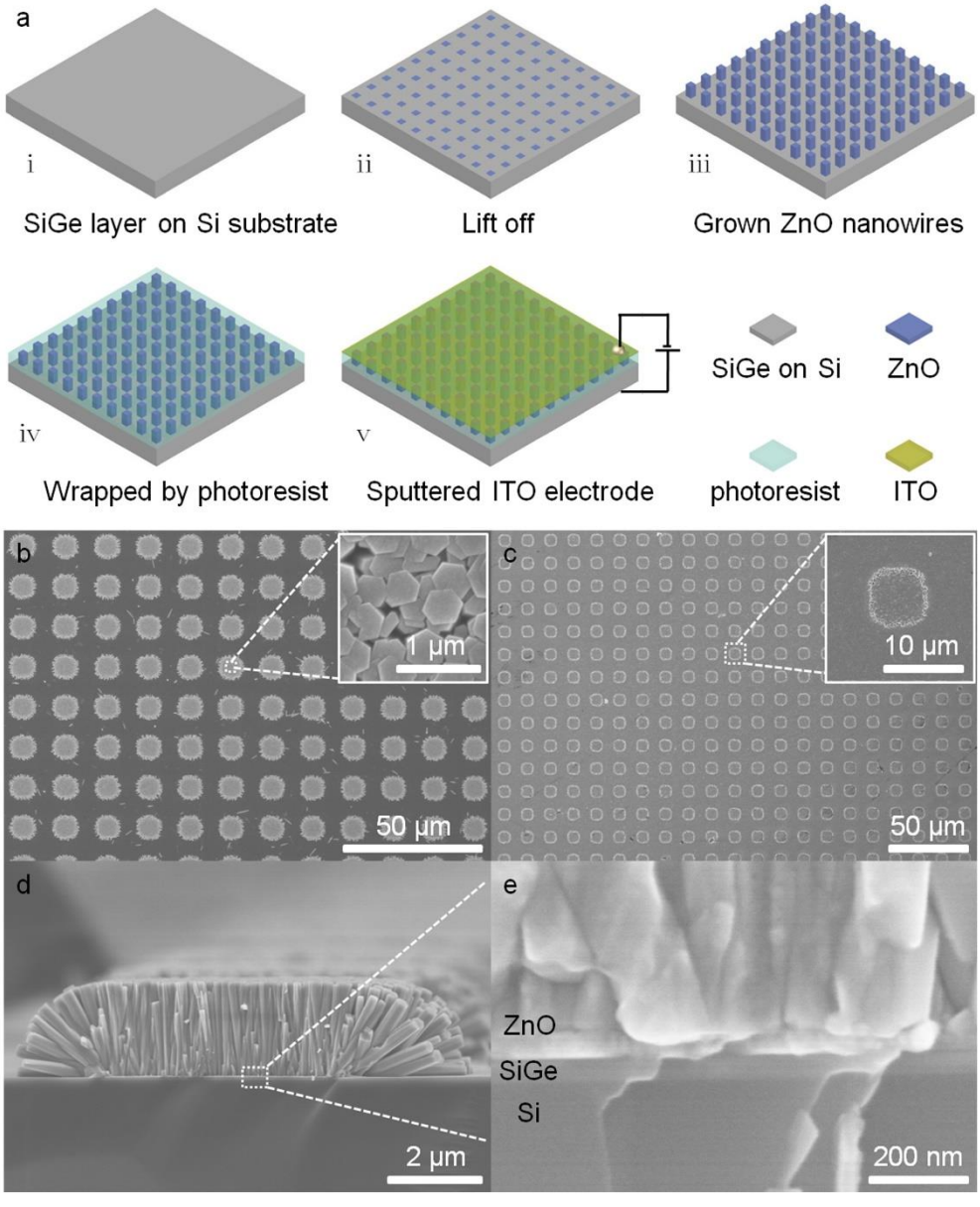

Figure 1 (a) Schematic of the device fabrication process. (b) Top SEM image of the as-grown ZnO nanowire pixels array on the SiGe alloy film; Insert: enlarged SEM image of the ZnO nanowires in the center of a pixel. (c) Top SEM image of ZnO nanowire/SiGe LEDs after the ITO layer deposited; Insert: enlarged SEM of one LED. (d) SEM image of transaction of a ZnO nanowire pixel on the SiGe alloy film. (e) Enlarged SEM image of interface of ZnO nanowire pixel and SiGe alloy film.

Figure 2

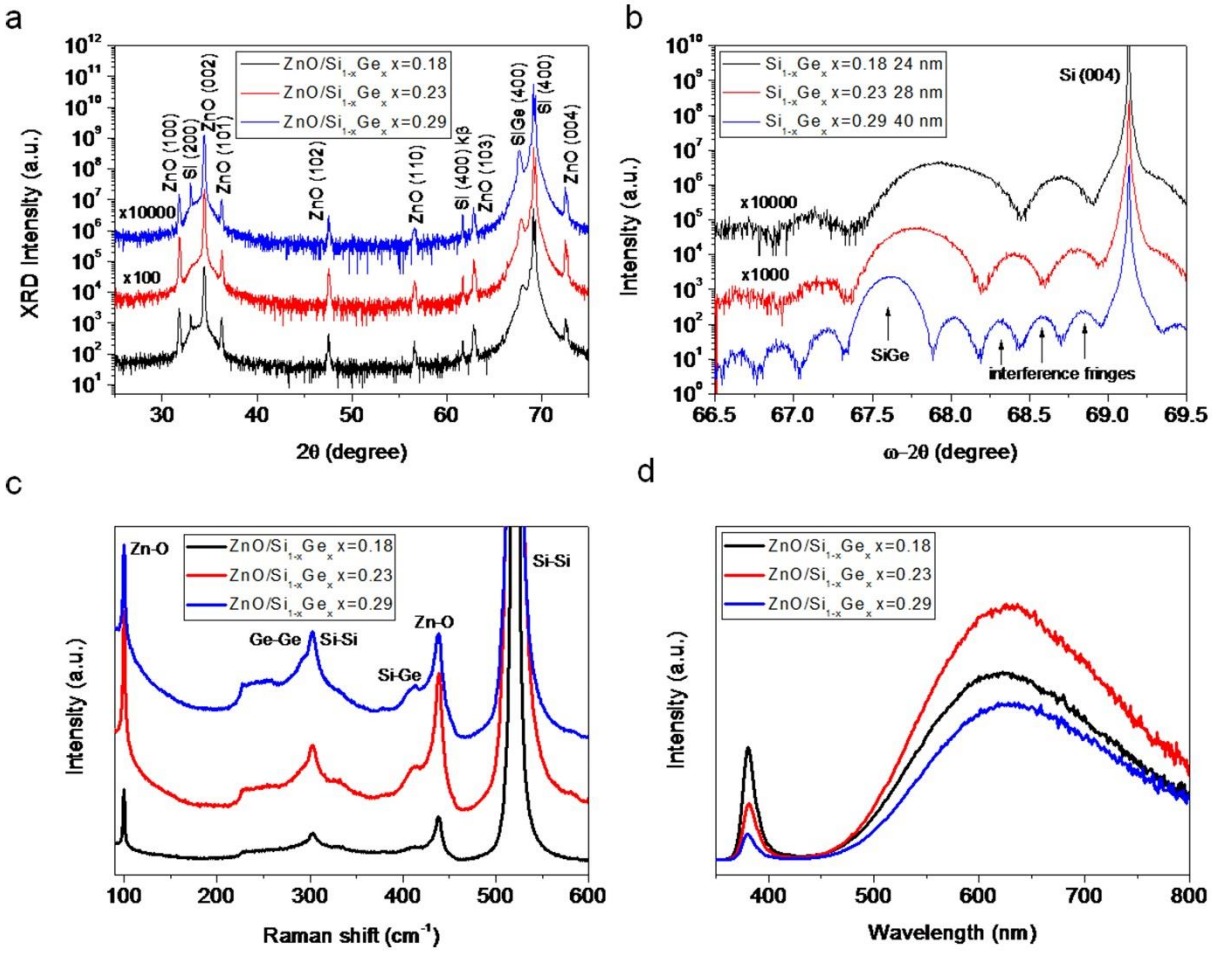

Figure 2 (a) XRD spectra of ZnO/SiGe nanoheterostructure array with Ge compositions 0.18, 0.23 and 0.29. (b) XRD rocking curves of SiGe layers with Ge compositions 0.18, 0.23 and 0.29. (c) Raman spectra of ZnO/SiGe nanoheterostructure array with Ge compositions 0.18, 0.23 and 0.29. (d) PL spectra of ZnO nanowires on the SiGe layers with Ge compositions 0.18, 0.23 and 0.29.

Figure 3

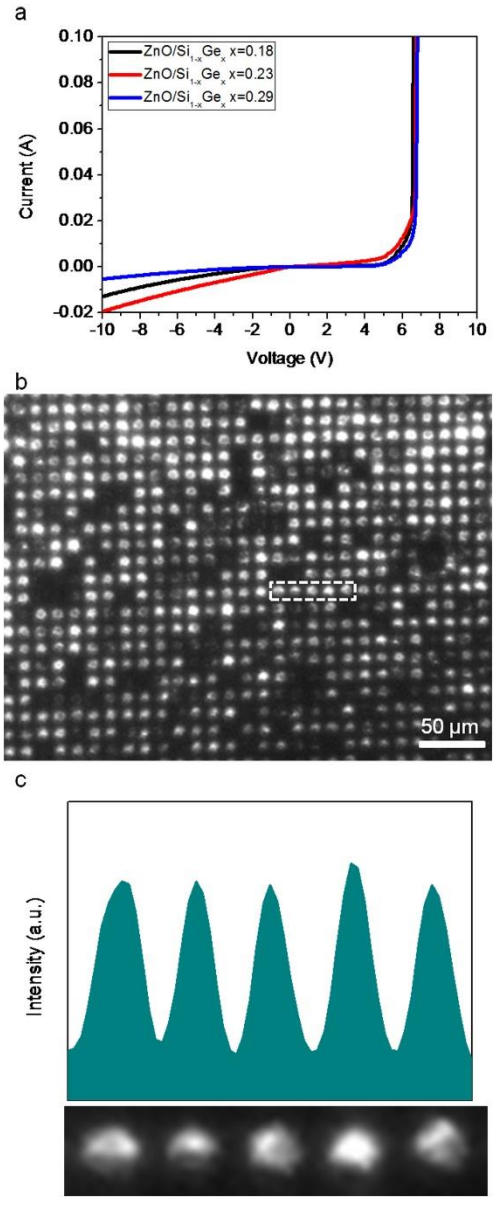

Figure 3 (a) Current-voltage (I-V) curves of three LEDs devices with Ge compositions 0.18, 0.23 and 0.29, the devices have the same size. (b) Optical image of a LEDs array when electrically emitting light by a applied current of 0.3 A, a nanowire pixel is a single LED that forms a pixel unit in the array. (c) Five typical LEDs (marked with a rectangle in (b)) and corresponding line profile of their emission intensity.

Figure 4

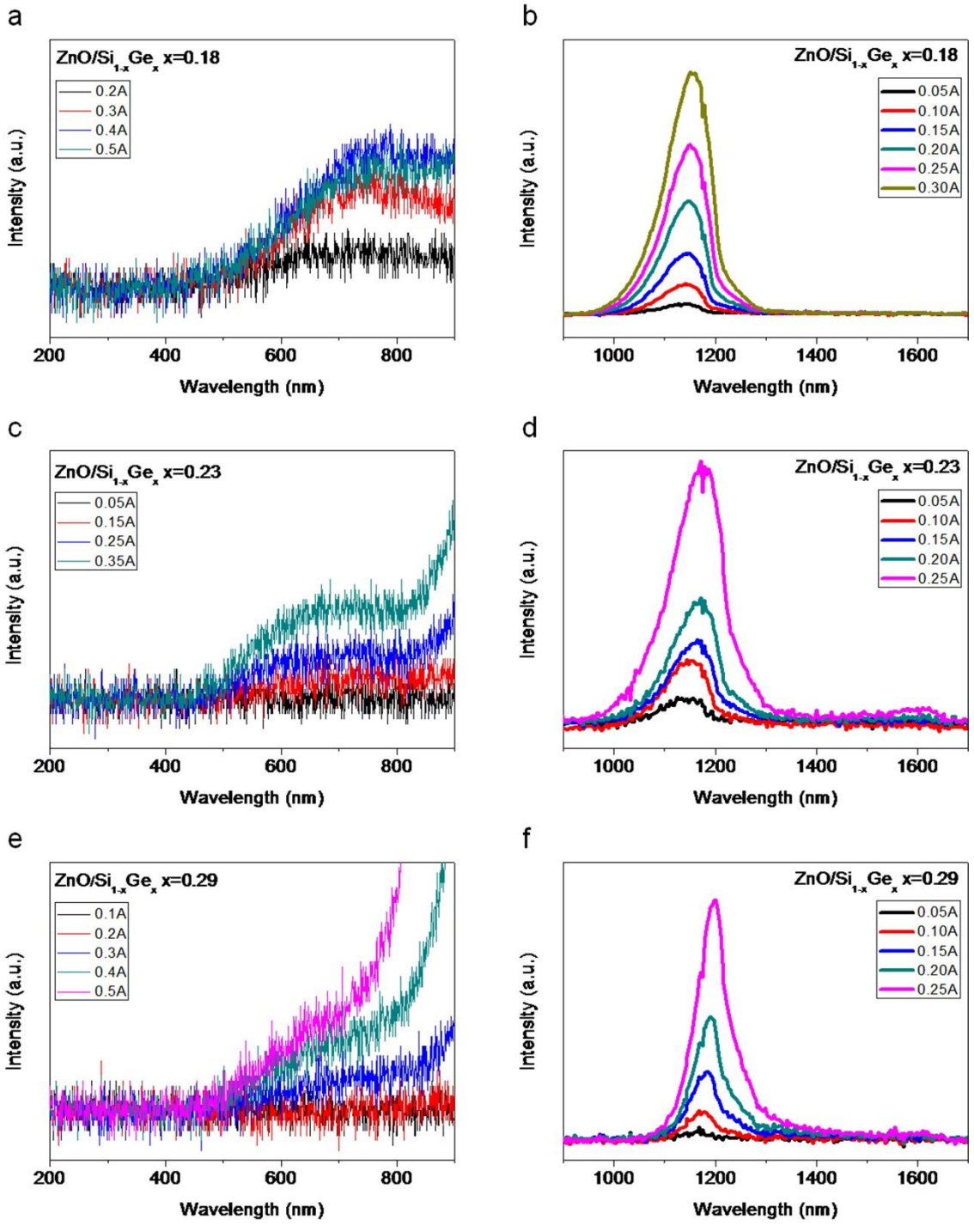

Figure 4 Electroluminescence spectra collected from three ZnO/SiGe LEDs devices with Ge compositions 0.18, 0.23 and 0.29. (a), (c) and (e) are in visible range. (b), (d) and (f) are in infrared range.

Figure 5

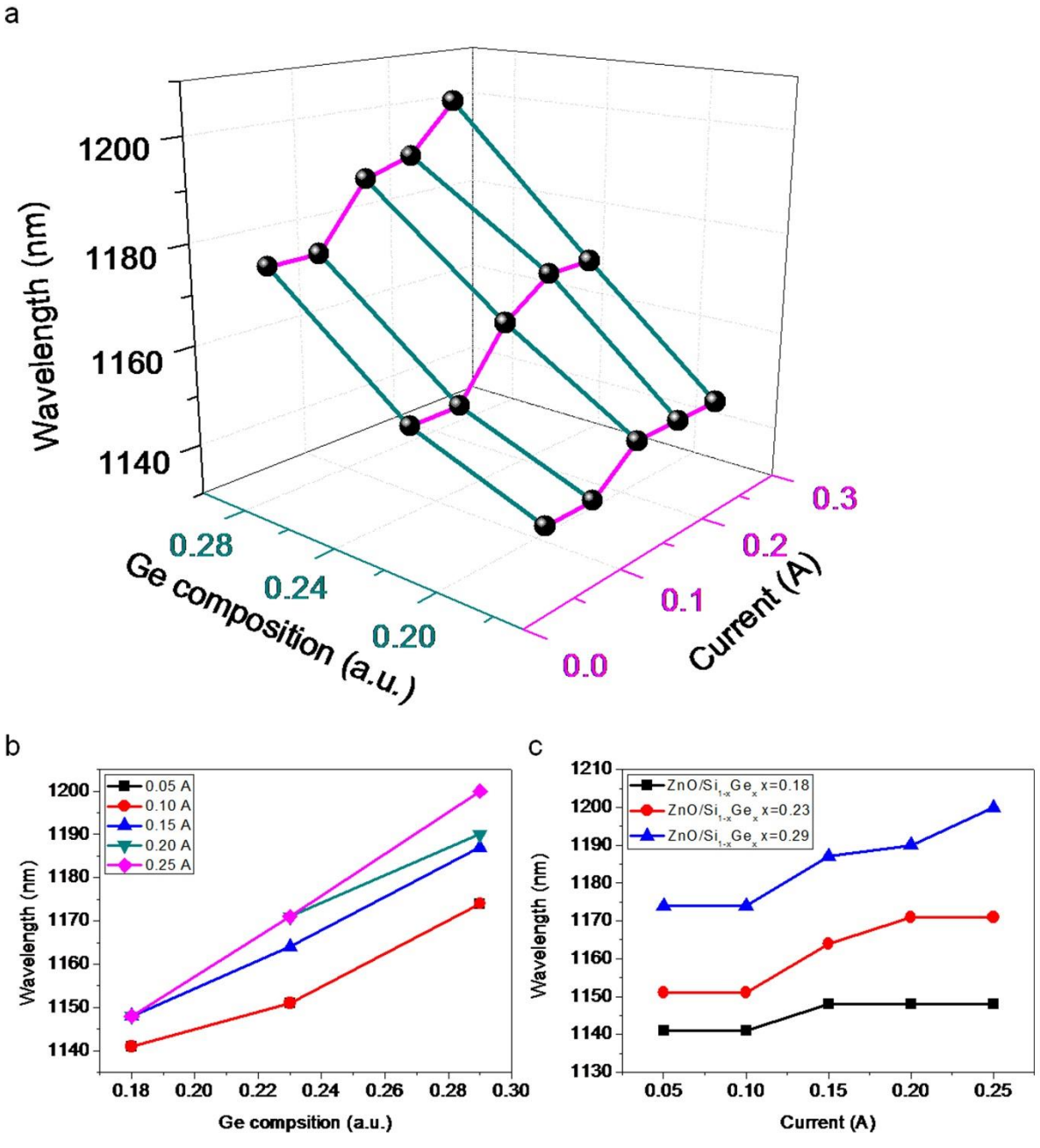

Figure 5 (a) 3D graph depicting the wavelength variation of the ZnO/SiGe LED under different applied currents and Ge compositions. (b) Wavelength variation of the ZnO/SiGe LED under different Ge compositions. (c) Wavelength variation of the ZnO/SiGe LED under different applied currents. Data of (b) (c) were extracted from (a).